Study on the liquid water sloshing in two- and three-dimensional models

Jianwei Zhang[a], Wanqing Wu[b] , Junquan Hu[c] and Bin Zhang[d]

Department of Marine Engineering, Dalian Maritime University, Dalian 116026, China;

[a]zjw220dlmu@163.com, [b]wuwanqingdmu@sina.com, [c]hujunquan@shmsa.gov.cn, [d]zhangbindlmu@hotmail.com

Keywords: Sloshing, Pressure, Sloshing-induced moment, CFD method, VOF method.

Abstract. Liquid sloshing in tanks has many important applications in a variety of engineering fields. In this study, based on a CFD solver, a numerical model is developed to study the liquid water sloshing in two- and three-dimensional tanks. The VOF method is used to capture the fluid interface. In order to validate the proposed model, a 2-D liquid-water sloshing problem was first solved. The variations of the pressure at the monitor point 100 mm below the initial free surface were recorded. Then the method was applied to a 3-D liquid-water sloshing problem and the sloshing-induced moment was obtained. The numerical results were compared and analyzed with experimental measurements. The results confirm that the present method can be adopted to predict the motion of liquid water and analyze its induced moment on the tank boundary when it has a roll motion.

Introduction

Liquid sloshing in tanks has gained considerable attention in transportation engineering during recent decades. Liquid motion in partially filled tanks can cause a larger impact loads if the period of excitation is close to the natural period of fluid inside the tank [1]. The amplitude of the impact pressure and the induced-moment depends on excitation amplitude and frequency of the tank motion, liquid-fill depth, liquid properties and tank geometry. The liquid water sloshing problem has been studied by many researchers and the several recent studies are summarized as follows.

Nasar et al. [2] carried out an experimental study to measure the pressures on the walls and on the top cover of a tank subjected to combined motions. In their study, four different liquid fill levels were considered and the effects of excitation frequencies and amplitudes on the pressure variation had been studied in detail. Brizzolara et al. [3] assessed four different numerical methods for sloshing evaluation. The impact pressures and global moment induced by water motion in a partially filled rectangular tank were predicted and compared with experimental measurements. Wu et al [4] investigated the hydrodynamic forces induced by transient sloshing in a 3-D rectangular tank by a time independent finite difference method. The evolutions of sloshing-induced forces of different types of sloshing waves were obtained, and the computational results were in good agreement with experimental measurements. Jung et al [5] analyzed the variation of pressure and the free surface elevation with respect to the baffle height in a three-dimensional tank based on the finite volume and the volume of fluid (VOF) methods. The computation was validated by the experimental results. Akyildiz [6] solved the complete Navier-Stokes equations using finite difference approximations and the volume of fluid technique, the effect of the vertical baffle heights on the liquid sloshing was studied. It denoted that the block effect of the baffle on the liquid convection is predominant to the tip vortex. Thiagarajan et al [7] studied the effects of excitation and fill levels on the air-water sloshing problem using a finite volume approximation and a linear potential theory. They pointed out that 20% and 80% fill levels had higher pressures than other conditions although resonance conditions were well-known to cause much higher loads. Furthermore, at fill levels beyond 50%, the maximum pressure occurred at a fixed point on the roof, which points to some topological effects of the free surface during the roof impact.

In this study, a numerical model based on a CFD solver is proposed to solve the 2-D and 3-D liquid water sloshing problem. The VOF tool is used to capture the fluid interface. The main purpose of this study is to assess the impact pressure and the sloshing-induced moment on the tank boundary under

different excitation modes. The variations of the pressure and the sloshing-induced moment were recorded and compared with experimental data or other published numerical results.

Mathematical background and numerical approach

Governing equations. The fluid is assumed to be homogenous, isotropic and viscous. The present liquid water sloshing problem assuming the flow is turbulent. Turbulent flows at realistic Reynolds numbers are characterized by a large range of length and time scales. The time averaging turbulence effects are incorporated in terms of the mean quantities of the flow, the instantaneous velocity is constituted by the mean and the fluctuating components of the velocity. So the incompressible flow is governed by the continuity and Reynolds-averaged Navier-Stokes (RANS) equations, written as follows:

$$\frac{\partial u_i}{\partial x_i} = 0 \tag{1}$$

$$\rho \frac{\partial u_i}{\partial t} + \rho u_j \frac{\partial u_i}{\partial x_j} = -\frac{\partial p}{\partial x_i} + \frac{\partial}{\partial x_j}\left[\mu\left(\frac{\partial u_i}{\partial x_j} + \frac{\partial u_j}{\partial x_i}\right)\right] + \frac{\partial}{\partial x_j}(-\rho\overline{u_i u_j}) + F_i \tag{2}$$

Where x_i are Cartesian coordinates, u_i are the corresponding velocity components. $\rho = \alpha\rho_1 + (1-\alpha)\rho_2$ is the mixture density, ρ_1 and ρ_2 are the density of water and the air, respectively. $\mu = \alpha\mu_1 + (1-\alpha)\mu_2$ is the mixture viscosity, μ_1 and μ_2 are the viscosity of water and the air, respectively. α is the fluid volume fraction, which is set to 1 in the water region, 0 in the air region and between 0 and 1 for the interface. F_i is the external body force, p is the pressure. Besides, $-\rho\overline{u_i u_j}$ is the Reynolds stress term, the equations are closed by the *RNG* $\kappa-\varepsilon$ turbulent model [8].

The volume of fluid (VOF) method is used to capture the free surface. The VOF formulation relies on that the two or more fluids are not interpenetrating and for each phase a variable, α, the volume fraction of the corresponding phase is introduced. The interface deformation is characterized by means of a scalar function, whose value is set based on the volume fraction of a computing unit. At each time step, the function is solved to find the distribution of the fluid phases. The equation governing α is as follows:

$$\frac{\partial \alpha}{\partial t} + u_i \frac{\partial \alpha}{\partial x_i} = 0 \tag{3}$$

And that the volume fraction equation is not solved for the primary phase, but the volume fraction of all phases sum to unity in each control volume and based on the following relationship:

$$\sum_{q=1}^{m} \alpha_q = 1 \tag{4}$$

Where α_q is the volume fraction of the *q*th fluid and m is the number of the phases.

By solving a single momentum equation throughout the domain and the resulting velocity field is shared among the phases [9]. In the case of turbulent quantities, the *RNG* $\kappa-\varepsilon$ transport equations are solved and the turbulent variables are shared by the phases throughout the field. The volume fraction transport equation is solved through implicit time discretization when transient calculation is considered.

Convection and diffusion terms are discretized using the second order upwind scheme and the second order accurate central differencing scheme, respectively. For unsteady flow calculations, time derivative terms are discretized using the first order accurate backward implicit scheme. The velocity-pressure coupling and overall solution procedure are based on PISO segregated algorithm adapted to an unstructured grid.

Sloshing-induced moment formulation. In present study, the moments produced by liquid water sloshing are discussed extensively. The sloshing moment can be obtained by the formulation as follows:

$$\overrightarrow{M}_A = \vec{r}_{AB} \times \overrightarrow{F}_p + \vec{r}_{AB} \times \overrightarrow{F}_v \tag{5}$$

Where A represents the specified moment center, B is the force origin, $\vec{r}_{AB}$ is the moment vector, $\overrightarrow{F}_p$ is the pressure force vector and $\overrightarrow{F}_v$ is the viscous force vector, respectively. And the pressure forces are calculated by following equation:

$$\vec{F}_p = \sum_{i=1}^{n} pA\hat{n} - p_{ref} \sum_{i=1}^{n} A\hat{n} \tag{6}$$

Where n is the number of faces, A is the area of the faces, $\hat{n}$ is the unit normal to the face, and p is the pressure of the faces. In order to reduce round-off error, a reference pressure (p_{ref}) is used to normalize the cell pressure for computing the pressure force. Further details of the formulations can be found in the ANSYS Fluent (2012) manuals [10].

Results and discussions

Sloshing of a 2-D basin under roll excitation. To testify the proposed method, it is applied to a 2-D sloshing problem. As shown in Fig. 1, the size of the basin is measured by $B \times H$, and the fluid (liquid water) depth is d.

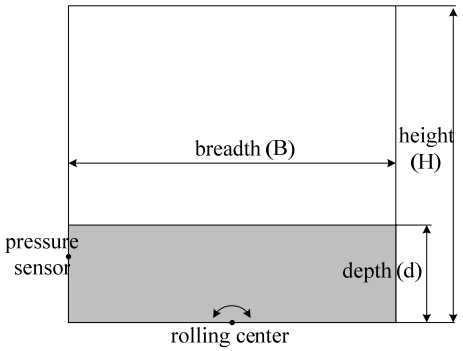

Fig. 1 The sketch of the 2-D basin model

For the given rectangular basin, the first natural frequency ω_0 can be obtained by:

$$\omega_0 = \sqrt{\frac{\pi g}{B} \tanh(\frac{\pi d}{B})} \tag{7}$$

Where g is the gravitational acceleration.

The basin has a roll motion around the axis at the center of the bottom. The roll angle displacement α is controlled by the form:

$$\alpha = A\sin(\omega t) \tag{8}$$

Where A, ω, t denote the rolling angle amplitude, the excitation circular frequency and time, respectively.

The dimension of the 2-D water basin are $B = 1000$ mm, $H = 1000$ mm, $d = 300$ mm and a pressure sensor is located 100 mm below the initial water free surface on the left solid boundary. According to Eq. (7), the first natural frequency and the corresponding period of the sloshing model are $\omega_0 = 4.76$ rad/s , $T_0 = 1.32$ s . The maximum rolling angle is set to $5°$. In order to investigate the sloshing phenomena extensively, four excitation frequencies are selected, one is far lower than the first natural frequency, two are a little smaller than the first natural frequency and the fourth is higher than the first natural frequency. They are $\omega_1 = 0.95$ rad/s , $\omega_2 = 3.09$ rad/s , $\omega_3 = 3.81$ rad/s and $\omega_4 = 5.47$ rad/s , respectively.

In the model, the quad grid is adopted for the computation. After carrying out the grid and the time step independence study, the size of a computing cell is set to 5 mm × 5 mm and the time step is set to 0.001s. The convergence criterion is below 1e-5 for the governing equations. The variation of pressure at the monitor point is the main focus. The pressure values presented in [11] and those obtained from present numerical method are compared. Figs. 2-5 show the pressure curves under the

four motivation modes. Comparing these figures, it can be seen that the oscillations of the pressure become more violent when the excitation frequency increases. At a lower excitation frequency, the pressure changes smoothly and stably, which is mainly caused by the static pressure of the liquid water. When the frequencies become higher, the violent water movement and the beating phenomenon take place. Around the resonance frequency, owing to that the water movement cannot follow the motion of the basin, there are always two successive peaks in each period of the pressure curves. The first peak caused by the initial impact. Then the liquid water swells up along the side boundary and the kinetic energy of the fluid decreases and the potential energy increases. Along with the continuously impacts the second peak occurs. It is found that, the present numerical results are in good agreement with the experimental and published results no matter in period or amplitude, validating the model presented above. There are still some inconsistent in pressure amplitude compared to the experimental data, which is due to the accumulation of numerical dissipations and 3D effects in experimental tests.

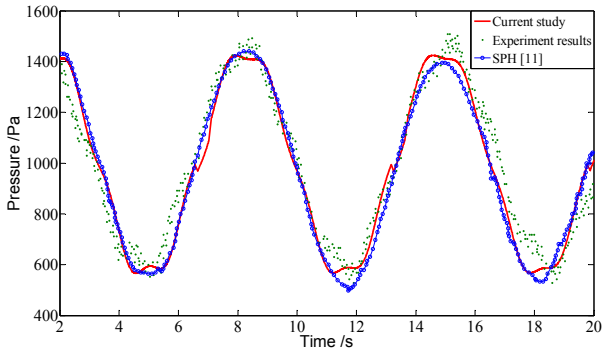

Fig. 2 Comparison of the pressure values at the monitor point ($\omega_1 = 0.95$ rad/s)

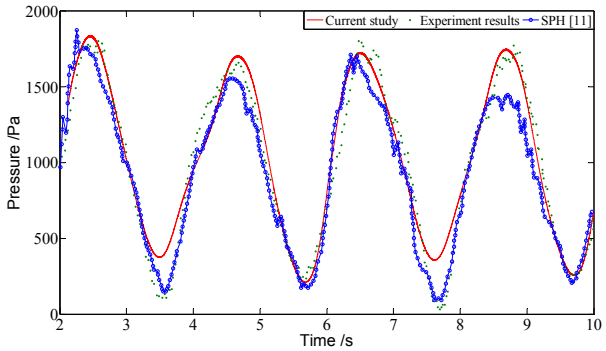

Fig. 3 Comparison of the pressure values at the monitor point ($\omega_2 = 3.09$ rad/s)

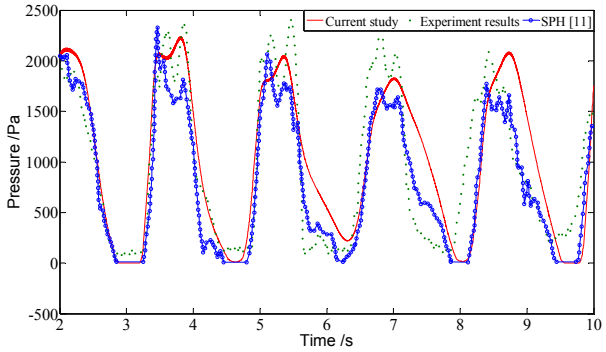

Fig. 4 Comparison of the pressure values at the monitor point ($\omega_3 = 3.81$ rad/s)

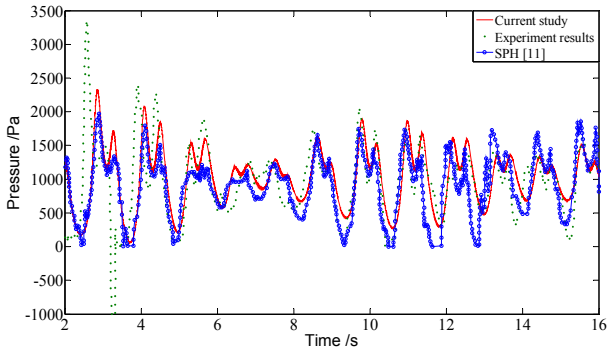

Fig. 5 Comparison of the pressure values at the monitor point ($\omega_4 = 5.47$ rad/s)

Sloshing of a 3-D tank under roll excitation. To further validate the accuracy of calculating the sloshing-induced force or moment in the model, a 3-D tank water sloshing problem of Iglesias [12] is simulated and the results are compared. The geometry of the 3-D tank model is shown in Fig. 6, the rectangular tank has a breadth of 640 mm, a height of 140 mm and a length of 252 mm. The tank model has a roll motion around a roll center which is 100 mm below its baseline. The roll amplitude is 6° and the angle of rotation in degree is $\alpha = 6\sin(\omega t)$. According to Eq. (7), the first natural frequency is $\omega_0 = 2.65$ rad/s. In Fig. 7, it can be seen that around the first resonance frequency the moment amplitude is up to the maximum. And the dramatic variations mainly happened in the stage between point A and B, corresponding to $\omega_A = 4.34$ rad/s and $\omega_B = 4.87$ rad/s. When the excitation frequency is higher than 4 rad/s, the movement of the liquid water is not synchronized with the tank, the left and right forward waves will clash with each other. The mass center of the water will not deviate a lot from the roll center, the moment amplitude caused by the liquid water decreases naturally.

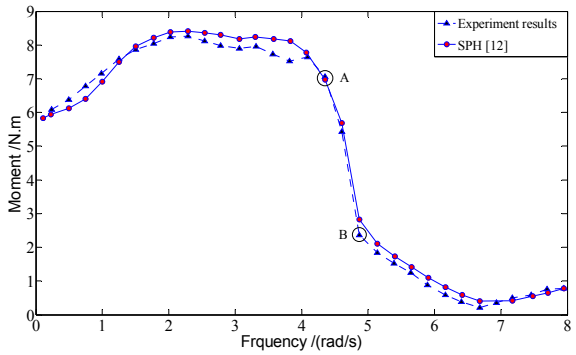

Fig. 7 The moment amplitude of experimental and SPH [12] results vs. excitation frequencies

The hexahedron grid is adopted here for the simulation. After carrying out the time and grid independence study in the context of this problem, the size of a compute cell is set to 10 mm × 10 mm × 14 mm, the time step is set to 0.005 s and the convergence criterion is below 1e-5 for the governing equations. In order to consider the efficiency and the comprehensiveness of the problem at the same time, four typical excitation frequencies are chosen to do the present calculation. They are 2.55 rad/s, 4.34 rad/s, 4.87 rad/s and 6.40 rad/s respectively. In each case, the simulation time runs up to ten periods. The comparison of the numerical results and the experimental data are shown in Figs. 8-11. In these four cases, the agreement is good. When the value of excitation frequency is about the same as the first resonance frequency of the sloshing system, the moment amplitude reaches the maximum. With increasing of the excitation frequency, the motion of the liquid water gradually lag behind the motion of the tank, so the moment amplitude decreases. In view of Fig. 9 and Fig. 10, the stable moment amplitude of point A is well agreement with the experimental and the SPH results in [12]. The moment variation of point B has a transient below 6 seconds and then a periodic response thereafter. Generally, the overall stable moment amplitudes are in good agreement with the

experiment tests. From the above analysis and comparison of the results achieved by different methods, it can be deduced that the simulation model and the moment calculation method used in this paper is reliable and accurate.

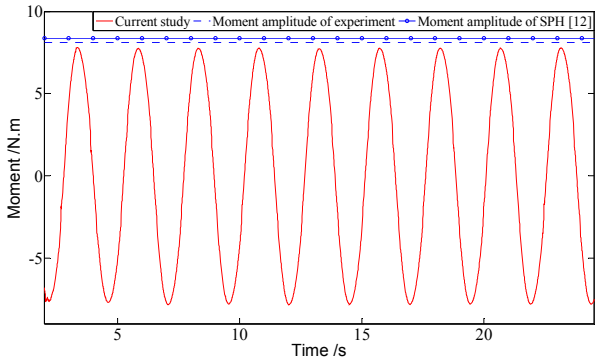

Fig. 8 Variation of moment at excitation frequency equals 2.55 rad/s

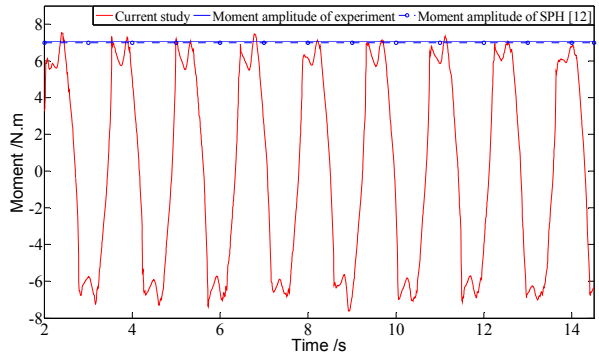

Fig. 9 Variation of moment at excitation frequency equals 4.34 rad/s

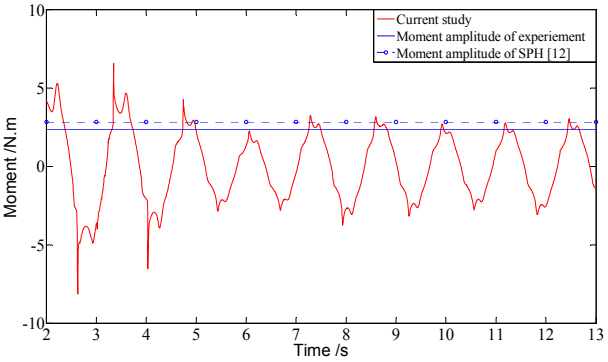

Fig. 10 Variation of moment at excitation frequency equals 4.87 rad/s

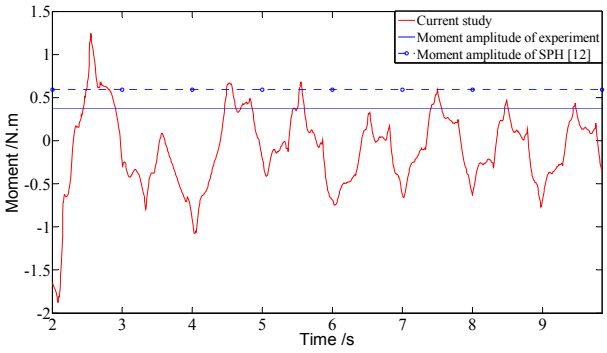

Fig. 11 Variation of moment at excitation frequency equals 6.40 rad/s

Conclusions

In this study, based on a CFD solver, a numerical model is developed to simulate the liquid water sloshing problem. To verify the present model, the 2-D and 3-D liquid-water sloshing problem are solved. The variations of the pressure at the monitor point and the sloshing-induced moment is obtained. The numerical results are in good agreement with the experimental results.

It can be concluded that, When the excitation frequency becomes closer to the natural frequency of the 2-D and 3-D liquid-water sloshing system, more violent sloshing phenomenon occurs and more crests and troughs happen in the curves of the pressure and moment. When the excitation frequency is higher than a certain value, the liquid water movement cannot follow the tank's rolling motion. After the initial impact, due to the continuously impacts and the climbing of the liquid water at the side boundary, the second peak happens in the pressure and the moment curves. Around the natural frequency of the sloshing system, the pressure and induced moment amplitude on the boundary reaches the peak value. Beyond the range of the resonance condition, the pressure and moment amplitude is very sensitive to the excitation frequency. And further work will be carried out to investigate the coupled motion of liquid water and vessels combined with the seakeeping problem.

Acknowledgements

The research work was financially supported by National Natural Science Foundation of China (51306026).

References

[1] O.M. Faltinsen, A.N. Timokha. Sloshing, Cambridge University Press, New York, 2009.
[2] T. Nasar, SA. Sannasiraj, V. Sundar, Sloshing pressure variation in a barge carrying tank, Ships Offshore Struct. 3 (2008) 185-203.
[3] S. Brizzolara, L. Savio, M. Viviani, Y. Chen, P. Temarel, N. Couty, S. Hoflack, L. Diebold, N. Moirod, AS. Iglesias, Comparison of experimental and numerical sloshing loads in partially filled tanks, Ships Offshore Struct. 6 (2011) 15-43.
[4] C.H. Wu, B.F. Chen, T.K. Hung, Hydrodynamic forces induced by transient sloshing in a 3D rectangular tank due to oblique horizontal excitation, Comput. Math. Appl. 65(8) (2013) 1163-1186.
[5] J.H. Jung, H.S. Yoon, C.Y. Lee, S.C. Shin, Effect of the vertical baffle height on the liquid sloshing in a three-dimensional rectangular tank, Ocean Eng. 44 (2012) 79-89.
[6] H. Akyildiz, A numerical study of the effects of the vertical baffle on liquid sloshing in two-dimensional rectangular tank, J. Sound Vib. 331(1) (2012) 41-52.
[7] K.P. Thiagarajan, D. Rakshit, N. Repalle, The air–water sloshing problem: Fundamental analysis and parametric studies on excitation and fill levels, Ocean Eng. 38(2-3) (2011) 498-508.
[8] V. Y, S.A. Orszag, S. Thangam, T.B. Gatski, C.G. Speziale, Development of turbulence models for shear flows by a double expansion technique, Phys. Fluids A. 4(7) (1992) 1510-1520.
[9] C.W. Hirt, B.D. Nichols, Volume of fluid (VOF) method for the dynamics of free boundaries, J. Comput. Phys. 39(1) (1981) 201-225.
[10] ANSYS/Fluent, Fluent User's Guide, (2012) Ansys Inc.
[11] Z. Chen, Z. Zong, H.T. Li, J. Li, An investigation into the pressure on solid walls in 2D sloshing using SPH method, Ocean Eng. 59 (2013) 129-141.
[12] A. Souto-Iglesias, L. Delorme, L. Perez-Rojas, S. Abril-Perez, Liquid moment amplitude assessment in sloshing type problems with smooth particle hydrodynamics, Ocean Eng. 33(11-12) (2006) 1462-1484.